Acceleration of aqueous nano-film evaporation by applying parallel electric field

Wang, Bing Bing; Zhang, Hao Han; Xu, Zhi Ming; Wang, Xiao Dong; Zhao, Qi; Yan, Wei Mon

Published in:
International Journal of Heat and Mass Transfer

DOI:
10.1016/j.ijheatmasstransfer.2019.04.042

Publication date:
2019

Document Version
Peer reviewed version

Acceleration of aqueous nano-film evaporation by applying parallel electric field: A molecular dynamics simulation

Bing-Bing Wang[1], Hao-Han Zhang[1], Zhi-Ming Xu[1], Xiao-Dong Wang[2*], Qi Zhao[3], Wei-Mon Yan[4**]

[1]School of Energy and Power Engineering, Northeast Electric Power University, Jilin 132012, China;

[2]Research Center of Engineering Thermophysics, North China Electric Power University, Beijing 102206, China;

[3]School of Science and Engineering, University of Dundee, Dundee DD1 4HN, U.K.

[4]Department of Energy and Refrigerating Air-Conditioning Engineering, National Taipei University of Technology, Taipei 10608, Taiwan.

Abstract: In this work, molecular dynamics simulation has been applied to investigate the influence of external electric field on the evaporation of the aqueous nano-film. The evaporation of the aqueous nano-film with 2240 water molecules and 50 NaCl on a gold (100) surface is analyzed at the electric fields with various intensities (0, 0.05, 0.1, 0.2 and 0.3 V nm^{-1}) and directions. The predictions show that the evaporation of aqueous film is remarkably enhanced when the electric field E_x=0.2 or 0.3 V nm^{-1} is parallel to the aqueous film surface. It is also noted that free ions in the aqueous film are accelerated under the action of the higher E_x and water molecules in the hydration shell move together with the ions due to the hydration effect. As a result, the interaction between water molecules decreases, which is responsible for increasing the evaporation of the aqueous film under the action of the higher E_x. While applying the electric field E_y= ± 0.3 V nm^{-1} perpendicular to the aqueous film, ions cannot be in accelerated motion due to the existence of a solid-liquid interface and a liquid-gas surface in *y*-direction. Therefore, the evaporation enhancement is much lower than that of the aqueous film under the action of the E_x.

Keywords: evaporation; aqueous nano-film; electric field; molecular dynamics simulation, hydration effect

***Corresponding Author:** Xiao-Dong Wang, Tel. and Fax: +86-10-62321277, E-mail: wangxd99@gmail.com

****Corresponding Author.** Wei-Mon Yan, Tel.: +886-972909259, E-mail: wmyan@ntut.edu.tw

Nomenclature

r	distance	Pe	average potential energy
q	electric charge	N_f	number of degrees of freedom
t	time	$n_{neighbor}$	neighbor molecule number
k	Boltzmann constant	σ	characteristic diameter
v	velocity	ε_0	vacuum permittivity
m	evaporation rate	ε	well depth of LJ potential
T	temperature	*Subscripts*	
E	electric intensity	i, j	ith and jth particle
Ke	average kinetic energy	x, y	x and y-direction

1. Introduction

Various microelectronic and nano-optoelectronic technologies have adopted an external electric field as a driving procedure, such as electrostatic painting and spraying [1], inkjet printing [2], nano-manufacturing [3], electrospinning [4] and others. The liquid evaporation under external electric fields is key fundamental process and higher evaporation rate is critical for many application fields. For instance, the rapid evaporation of the solvent during the electrospinning process is essential to the forming of quite fine fibers with nanometer-scale diameters. But the reason for fast evaporation during electric field application is not yet understood well. Until now, the influence of external electric fields on the liquid film evaporation has generated much research interest towards developing a better understanding of the evaporation and localized interaction between liquid molecules under the action of the electric field.

Water is one of the most common working mediums, and water has dipolar molecules and its behavior can be affected by the electric field. Therefore, many researchers examined the liquid water evaporation under the action of the electric field by practical experience [5], theoretical analysis [6] and molecular dynamics (MD) simulation [7-10]. The MD simulation has an excellent track record of following molecule motions and localized interactions between molecules through the basic laws of classical mechanics, which is a powerful tool for microscopic analysis of water evaporation behaviors. Vaitheeswaran et al. [7] adopted the MD simulation to study of water behaviors between the plates at narrow separation in the presence of an electric field in an open system and they found that the evaporation of water was enhanced by applying high electric fields. The simulation suggested that the free energy barrier for water evaporation was reduced by the applied electric field. Okuno et al. [10] carried out a water nano-film evaporation simulation in the presence of electric fields with the value of 1 V nm^{-1} in three directions. The MD results disclosed that the electric field in the direction perpendicular to the film surface enhanced the water evaporation, while the electric field in the direction parallel to the water surface impeded the water evaporation. This can be made plausible by noting the fact that the water dipolar alignments under the action of electric fields in various directions are different.

In practical terms, the water film generally dissolved the free ions (aqueous film). When applying an electric field to the aqueous film, not only the water molecules but also the free ions

with charges were under the action of the electric force, which might be the reason that the evaporation of the aqueous film differed from the water film. Peng et al [11] adopted MD simulations to study the rupture and evaporation of aqueous nano-films with dissolved NaCl salt in the presence of external electric field. The electric fields in the direction perpendicular to the film surface were examined with the field intensity ranging from 0.1 to 10 V nm^{-1}. They found that the salts ions enhanced the rupture of water films at the absence of electric field and the rupture and water evaporation were accelerated with the increase of the electric field. The surface tension exhibited a decreasing trend with the increase of field strength. However, the effect of electric fields parallel to the aqueous nano-film surface on the evaporation was not discussed in their work. The aqueous nano-film had the liquid-gas or liquid-solid interface in direction perpendicular to the film surface, which differed from the one in the direction parallel to the film. As a result, applying electric fields in various directions might cause the difference of evaporation. According to our literature search, there is no study focusing on the effect of electric field direction on the evaporation of aqueous film and the effect of salts ions on the evaporation rate evolution under the action of the electric field, which has been considered worthy of the detailed analysis.

The objective of this work is to understand and reveal the difference of the aqueous film evaporation at homogeneous electric fields in three directions and to analyze the effect of ions on the evaporation rate of the aqueous films. Evaporation of an aqueous nano-film with dissolved 25, 50, or 100 NaCl was simulated at the lower electric fields (0, 0.05, 0.1, 0.2 and 0.3 V nm^{-1}), and the results show that the effect of the electric fields on the evaporation enhancement of the aqueous films with dissolved 25, 50, and 100 NaCl are similar. Thus, the evaporation behavior of the aqueous nano-film with dissolved 50 NaCl was analyzed in this paper. Water nano-film was also simulated for the comparative analysis. To reveal the evaporation difference, the motions of ions and water molecules as well as the interaction of water molecules were described in details. In addition, the evaporation of two thicker aqueous nano-films were built and simulated to prove the influence of electric field on the aqueous nano-film evaporation. The qualitative analysis of the MD trajectories provides molecular motion details, which is potentially useful for electric field design in order to enhance the evaporation of aqueous films in the actual application.

2. Model and Simulation

2.1 Model

The initial configuration of the system is shown in Fig. 1. The simulation box was cuboid with dimensions of 10.0×3.6×3.6 nm^3. The box was divided into three regions, namely solid, liquid and vapor regions. A gold (100) plate with 1.2 nm thickness and 972 gold atoms was modeled by the face-centered cubic (FCC) unit with a lattice constant of 0.408 nm. The gold plate consisted of six layers, the bottom layer was fixed to prevent the plate deformation [12] and other five layers were modeled as thermostat. An aqueous nano-film with 5.7 nm thickness was placed on the plate, and the nano-film consisted of 2240 water molecules and 50 Na^+ ions and 50 Cl^- ions. Periodical boundary conditions were applied to *x*- and *z*-direction of the box, while a fixed boundary condition was assumed in the *y*-direction. During the nano-film evaporation, the pressure of simulation box gradually increased which reduced the evaporation rate. To eliminate the effects of the pressure on the evaporation, the vapor region with 1.0 nm thickness at the top of the box was defined, and the gas water molecules were eliminated out the simulation box when the water molecules arrived at this region.

2.2 Potential function

The embedded atom model (EAM) [13] was adopted for simulating the interaction between gold atoms. The extended simple point charge (SPC/E) water model was chosen because it adequately captured the properties of liquid water in MD simulations [14]. The O-H bond length of 0.1 nm and the H-O-H angle of 109.47° were fixed with the method of the SHAKE algorithm [15]. Na^+ and Cl^- ions were modeled as charged Lennard-Jones particles [16, 17]. The interaction of water molecules and ions consisted of the Lennard-Jones 12-6 and Coulombic potentials were expressed as,

$$U_{ij} = 4\varepsilon_{ij}\left[\left(\frac{\sigma_{ij}}{r_{ij}}\right)^{12} - \left(\frac{\sigma_{ij}}{r_{ij}}\right)^{6}\right] + \frac{q_i q_j}{4\pi\varepsilon_0 r_{ij}} \quad (1)$$

where U_{ij} and r_{ij} are the potential energy and distance between particles *i* and *j*, q_i is the electric charge associated with site *i*, ε_0 is the vacuum permittivity, ε_{ij} is the well depth of the LJ potential, and σ_{ij} is the characteristic diameter. The interaction between the gold and other molecules (water,

Na^+ and Cl^-) was modeled by the Lennard-Jones 12-6 potentials. The values of parameters for the interactions are shown in Table 1. The potential parameters between different particles were described by the mixing rules, i.e., $\sigma_{ij} = (\sigma_i + \sigma_j)/2$, and $\varepsilon_{ij} = (\varepsilon_i \varepsilon_j)^{1/2}$. A spherical truncated distance for short-range forces was taken as 10 Å. The long-range electrostatic interaction was solved by PPPM (particle-particle particle-mesh) method [18] with a relative error of 10^{-4}.

2.3 Evaporation simulation

Before the onset of evaporation, the aqueous nano-film and the gold plate were simulated in an NVT ensemble at T=298 K to reach the equilibrium state using LAMMPS (large-scale atomic/molecular massively parallel simulator) [19]. A run of 1000 ps was made to ensure the equilibrium of the simulation system, and the electric field strength, E, was set to 0 V nm^{-1} during the equilibrium run. After the preparation of equilibrium system, the value of the homogeneous electric field was set to 0, 0.05, 0.1, 0.2 or 0.3 V nm^{-1} at x- and y-directions to investigate the effect of the electric field on the aqueous film evaporation. To trigger the evaporation, the temperature of gold atoms in the heat source rose rapidly up to 500 K by a Nose-Hoover thermostat [20, 21]. In the simulations, the particles motion was solved by the velocity-Verlet algorithm [22] with a time step of 1 fs, the positions and velocities of the particles were stored every 2 ps to analyze the results. Water molecules were considered to be in the liquid film if their neighbor molecule number within a distance of 4.34 Å, $n_{neighbor} \geq 4$, and in the vapor phase if $n_{neighbor} < 4$ [8].

The snapshots of the aqueous film evaporation at different instants for E=0 V nm^{-1} are presented in Fig. 2. When the gold plate temperature was suddenly increased from 298 to 500 K at t=0 ps, the nano-film was heated. An obvious thermal expansion of the aqueous film was observed at t< 320 ps. The thickness of the water film decreased with the aqueous film evaporation at t>320 ps. Finally, only a few water molecules absorbed the gold plate and the evaporation nearly completed at t=6000 ps, and the Na^+ and Cl^- ions were located on the gold surface with the morphology of crystal-like NaCl.

3. Results and discussions

Figure 3(a) shows the temporal evolution of number of evaporated water molecules and Figure

3(b) shows the evaporation rate (m) of aqueous film at the electric fields E_x=0, 0.05, 0.1, 0.2 and 0.3 V nm^{-1}. Here, the evaporation rate was equal to the quality of evaporated water molecules in each picosecond. Aqueous film was heated by the gold plate with high temperature of 500 K at t>0 ps, several water molecules evaporated in the initial stage as shown in Fig. 3(a). After that, more and more water molecules evaporated, and the number of evaporated water molecules was 2000 at t=5788 ps for the aqueous film at absence of the electric field. However, for aqueous film at the E_x=0.05, 0.1, 0.2 and 0.3 V nm^{-1}, evaporation of 2000 water molecules occurred at t=5576, 5076, 3128 and 1924 ps, respectively. The results indicated that evaporation of the aqueous film increased with the increase in electric field E_x.

As shown in Fig. 3(b), the evaporation rate increased at first and got maintained an average value of 1.10×10^{-26} kg ps^{-1} for the aqueous film at E_x= 0 V nm^{-1}. The evaporation rate increased to average values of 1.13×10^{-26} kg ps^{-1} and 1.19×10^{-26} kg ps^{-1} for the aqueous film at E_x=0.05 and 0.1 V nm^{-1}, respectively, which was slightly larger than the aqueous film at E_x= 0 V nm^{-1}. However, the evaporation rate remarkably increased at t<800 ps and t<580 ps for the aqueous film at E_x=0.2 and 0.3 V nm^{-1}, and decreased at t>800 ps and t>580 ps, respectively. The peak values were 3.15×10^{-26} kg ps^{-1} and 6.29×10^{-26} kg ps^{-1}, and the maximum of evaporation rate increased 2.83 and 5.67 times compared with the aqueous film at E_x= 0 V nm^{-1}.

For comparing and analyzing effect of electric field on the aqueous film evaporation, the evaporation behaviors of pure water nano-film at the electric fields E_x=0, 0.05, 0.1, 0.2 and 0.3 V nm^{-1} were simulated, and the number of evaporated water molecules versus time is presented in Fig. 4. The evaporation was not significantly different for the water film at E_x=0, 0.05, 0.1, 0.2 and 0.3 V nm^{-1}. The number of evaporated water molecules was 2113 and 2047 at t=6000 ps for the water film at E_x=0, 0.3 V nm^{-1}, respectively, which indicated that the evaporation rate decreased slightly for the pure water film at the stronger electric field E_x= 0.3 V nm^{-1}. These results agreed with the earlier studies of Okuno et al. [10], in which they found that the evaporation of thin pure water film decreased by applying E_x=1 V nm^{-1}. Consequently, it can be inferred that the increasing of the aqueous film evaporation rate by applying E_x should be attributed to the existence of ions in the nano-film.

To reveal the mechanisms behind the enhancement of aqueous film evaporation caused by applying the electric field E_x, average kinetic energy (Ke_{water}) of a liquid water molecule in nano-

film at different evaporation instants are shown in Figs. 5(a) (water film) and 5(b) (aqueous film). The film was heated by the gold surface, as the results that Ke_{water} was increasing for liquid water molecules in the water film or the aqueous film at the initial stage. While the Ke_{water} was kept a constant of 0.123 eV at t>420 ps, and the corresponding water temperature was 458.18 K calculated by the total kinetic energy of liquid water molecules as based on Eq. (2).

$$\frac{1}{2}N_f kT = \sum \frac{1}{2}m_i v_i^2 \quad (2)$$

Where N_f is the total number of degrees of freedom of water molecules, k is Boltzmann constant. $1/2m_i v_i^2$ is the kinetic energy of the ith water molecule, which contains the translation and rotational kinetic energy of water molecule. The results showed that the thermal energy does not increase the kinetic energy of liquid water molecule during t>420 ps and was only used to drive the water evaporation. In addition, it is shown in Fig. 5(a) that the value of Ke_{water} was not distinctly different with each other for the water films at E_x=0, 0.05, 0.1, 0.2 and 0.3 V nm^{-1}. However, the Ke_{water} has a remarkable increase at t<800 ps and t<580 ps for the aqueous film at E_x=0.2 and 0.3 V nm^{-1}, and decreased at t>800 ps and t>580 ps, respectively. There were peak values of 0.14 eV and 0.15 eV which were remarkably larger than the ones at E_x=0 V nm^{-1}.

To illustrate the reason of larger Ke_{water} for the aqueous film caused by application of the electric field E_x=0.2 and 0.3 V nm^{-1}, average kinetic energies (Ke_{Na^+} and Ke_{Cl^-}) of ions in aqueous film versus time are counted and shown in Figs. 6(a) and 6(b). When applying the electric field, Na^+ and Cl^- ions were accelerated and moved towards the direction of electric field, hence, the Ke_{Na^+} and Ke_{Cl^-} increased at t<800 ps and t<580 ps for E_x=0.2 and 0.3 V nm^{-1}, respectively. When NaCl was dissolved in the water film, some water molecules were bound by Na^+ and Cl^- ions due to the hydration effect [23]. Water molecules in the solvation shell moved together with the Na^+ and Cl^- ions leading to the increased Ke_{water} [9], which was responsible for the larger Ke_{water} when applying the higher electric field E_x=0.2 and 0.3 V nm^{-1} to the aqueous film.

In addition, ion pair formation for Na^+ and Cl^- ions existed in the aqueous film due to the Coulomb attractive force between opposite charges. Since the ion pair is intrinsically electroneutral, the electric field had a very small effect on the movement of the ion pair for Na^+ and Cl^-. A concept of critical distance between Na^+ and Cl^- is a benchmark to evaluate whether the ion pair is formed or not [24]. During the process of the evaporation, the volume of aqueous film decreased and the

concentration of Na^+ and Cl^- ions in the aqueous film increased, and more ion pairs were formed for Na^+ and Cl^- ions [25], which lead to the number of free ions reduction. Thus, the Ke_{Na^+} and Ke_{Cl^-} as well as Ke_{water} reduced gradually at final stage (t>800 ps and t>580 ps) for E_x=0.2 and 0.3 V nm^{-1} as shown in Fig.5(b) and Fig.6.

The average potential energy of liquid water molecules (Pe_{water}) was calculated by average interaction between each water molecule and other molecules in the liquid film (include Na^+ and Cl^- ions for aqueous film) and the results are shown in Fig. 7. The negative value of Pe_{water} denoted an attractive interaction, which was stronger for a larger absolute value. The value of Pe_{water} was 0.43 eV at t=0 ps. The Pe_{water} decreased during the thermal expansion of the liquid film in the initial heating stage, and the Pe_{water} decreased to an average constant of 0.37 eV at t>780 ps. The values of Pe_{water} were not remarkably different for the water film at E_x=0, 0.05, 0.1, 0.2 and 0.3 V nm^{-1} as shown in Fig. 7(a).

As noticed in Fig. 7(b), the Pe_{water} varied with each other for the aqueous film at E_x=0, 0.05, 0.1, 0.2 and 0.3 V nm^{-1}. The value of Pe_{water} decreased to a lower value for the aqueous film by applying the higher electric field E_x (eg. E_x= 0.2 or 0.3 V nm^{-1}), which indicated that the interaction between water molecules in the aqueous film decreased under the action of electric field E_x. Thus, the water molecules escaped from the aqueous film more easily. The variation of Pe_{water} versus time was related to the kinetic energy of water molecules as shown in Fig. 5(b). In summary, ions were accelerated by the higher electric field and the water molecules were forced to move together with the ions. As a result of the decrease of the interaction between water molecules, which was responsible for the enhancement of the aqueous film evaporation by applying the higher electric field E_x.

The aqueous film evaporation was remarkably improved by the application of stronger electric fields parallel direction to the aqueous film surface, which was attributed to the ions accelerated motion along the direction of electric field. A solid-liquid interface and a liquid-gas surface existed in y-direction for the aqueous film as shown in Fig.1, which differed from the aqueous film at x-direction. Therefore, the evaporation of the aqueous film was discussed at the electric field in the direction perpendicular to the aqueous film surface. The numbers of water molecules evaporated versus time for aqueous film at E=0 V nm^{-1}, E_x=0.3 V nm^{-1}, E_y=+0.3 V $nm^{-1}$and E_y=-0.3 V nm^{-1} are shown in Fig.8. The evaporation of 2000 water molecules occurred at 5788, 1924, 5464 and 5516

ps for aqueous film at E=0.0 V nm^{-1}, E_x=0.3 V nm^{-1}, E_y=+0.3 V nm^{-1}and E_y=-0.3 V nm^{-1}, respectively. The results showed that the aqueous film evaporation rate increased slightly by the application of electric field E_y=+0.3 V nm^{-1}or E_y=-0.3 V nm^{-1}, which was remarkably lower than the evaporation rate of the aqueous film at E_x=0.3 V nm^{-1}. Average kinetic energies (Ke_{Na^+} and Ke_{Cl^-}) of ions in aqueous film versus the evaporation time are shown in Figure 9. The Na^+ and Cl^- ions were not accelerated by applying E_y=±0.3 V nm^{-1} due to the limitation of the solid-liquid interface and the liquid-gas surface in the *y*-direction.

Two thicker aqueous nano-films were built in order to verify the effect of electric field on the evaporation of aqueous film. One aqueous film had 2240 water molecules with dimensions of 2.4×12.8×2.4 nm^3, and 50 Na^+ ions and 50 Cl^- ions were dissolved in the aqueous film. Another aqueous film had 3360 water molecules with dimensions of 2.4×19.2×2.4 nm^3, and 75 Na^+ ions and 75 Cl^- ions were dissolved in the aqueous film. The evaporation was also triggered by the heat source with the high temperature of 500 K. The numbers of water molecules evaporated versus time for aqueous film with 12.8 nm and 19.2 nm thicknesses at E=0.0 V nm^{-1}, E_x=0.1 V nm^{-1}, E_y=+0.1 V nm^{-1}and E_y=-0.1 V nm^{-1} were shown in Fig. 10(a) and 10(b), respectively. Evaporation of 2000 water molecules occurred at 24100, 13370, 22710 and 21200 ps for aqueous film with 12.8 nm thickness at E=0.0 V nm^{-1}, E_x=0.1 V nm^{-1}, E_y=+0.1 V nm^{-1}and E_y=-0.1 V nm^{-1}, respectively. While evaporation of 3000 water molecules occurred at 46350, 15130, 42190 and 37110 ps for aqueous film with 19.2 nm thickness, respectively. The results showed that the thicker aqueous films evaporation was remarkably enhanced by applying E_x=0.1 V nm^{-1}, and the evaporation rate of aqueous film at E_y=-0.1 V nm^{-1} was larger than the ones at E_y=+0.1 V nm^{-1}, which were consistent with the above mentioned conclusions. In addition, different growth evaporation rates for the three aqueous films exist when applying E_x=0.1 V nm^{-1}: The evaporation increased by 12.3 % {=(5788-5076)/5788} for 5.7 nm aqueous film as shown in Fig. 3(b), while the evaporation rate increased by 44.5 % {=(24100-13370)/24100} and 67.4 % {=(46350-15130)/46350} for 12.8 nm and 19.2 nm aqueous film, respectively. The results showed that the evaporation enhancement is much higher for the thicker aqueous nano-film when applying E_x=0.1 V nm^{-1}.

4. Conclusions

In summary, the effects of the electric field on evaporation of the aqueous nano-films with two various thicknesses were investigated via molecular dynamics simulations. The predictions showed that the evaporation of aqueous film was remarkably enhanced while applying a high electric field parallel to the surface of aqueous film (E_x). It was inferred that water molecules in the solvation shell moved together with the ions under action of the higher electric field E_x, as a result that the interaction between water molecules decreased, which was responsible for increasing the evaporation of the aqueous film under the action of the electric field E_x. While applying an electric field (E_y) perpendicular to the aqueous film, the evaporation enhancement was lower than that of the aqueous film under the action of the E_x, because ions cannot be in accelerated motion due to the existence of a solid-liquid interface and a liquid-gas surface in the direction perpendicular to the aqueous film surface.

Acknowledgments

This study was supported by The National Natural Science Foundation of China (No. 51706038) and The National Science Fund for Distinguished Young Scholars of China (No. 51525602).

References

[1]. M. Barletta, A. Gisario, Electrostatic spray painting of carbon fibre-reinforced epoxy composites, Prog. Org. Coat. 64 (2009) 339-349.

[2]. T.G. Twardeck, Effect of parameter variations on drop placement in an electrostatic ink jet printer, IBM. J. Res. Dev. 21 (1977) 31-36.

[3]. X. Liang, W. Zhang, M. Li, Q. Xia, W. Wu, H. Ge, X. Huang, S.Y. Chou, Electrostatic force-assisted nanoimprint lithography, Nano. Lett. 5 (2005) 527-530.

[4]. J.S. Choi, S.W. Lee, L. Jeong, S.H. Bae, B.C. Min, J.H. Youk, W.H. Park, Effect of organosoluble salts on the nanofibrous structure of electrospun poly (3-hydroxybutyrate-co-3-hydroxy-Valerate), Int. J. Biol. Macromol. 34 (2004) 249-256.

[5]. K. Takano, I. Tanasawa, S. Nishio, Active enhancement of evaporation of a liquid drop on a hot

solid surface using a static electric field, Int. J. Heat Mass Transfer. 37 (1994) 65-71.

[6]. N. Sharma, G. Diaz, E. Leal-Quirós, Electrolyte film evaporation under the effect of externally applied electric field, Int. J. Therm. Sci. 68 (2013) 119-126.

[7]. V. Subramanian, Y. Hao, J.C. Rasaiah, Water between plates in the presence of an electric field in an open system, J. Phys. Chem. B. 109 (2005) 6629-6635.

[8]. B.B. Wang, X.D. Wang, Y.Y. Duan, M. Chen, Molecular dynamics simulation on evaporation of water and aqueous droplets in the presence of electric field, Int. J. Heat Mass Transfer. 73 (2014) 533-541.

[9]. B.B. Wang, X.D. Wang, T.H. Wang, Microscopic mechanism for the effect of adding salt on electrospinning by molecular dynamics simulations, Appl. Phys. Let. 105 (2014) 121906.

[1]. Y. Okuno, M. Minagawa, H. Matsumoto, A. Tanioka, Simulation study on the influence of an electric field on water evaporation, J. Mol. Struc-Theochem. 904 (2009) 83-90.

[2]. T. Peng, Q. Li, C. Liu, Accelerated aqueous nano-film rupture and evaporation induced by electric field: A molecular dynamics approach, Int. J. Heat Mass Transfer. 94 (2016) 39-48.

[3]. B.B. Wang, X.D. Wang, T.H. Wang, G. Lu, W.M. Yan, Enhancement of boiling heat transfer of thin water film on an electrified solid surface, Int. J. Heat Mass Transfer. 109 (2017) 410-416.

[4]. S.M. Foiles, M.I. Baskes, M.S. Daw, Embedded-atom-method functions for the fcc metals Cu, Ag, Au, Ni, Pd, Pt, and their alloys, Phys. Rev. B. 33 (1986) 7983-7991.

[5]. P. Varilly, D. Chandler, Water evaporation: A transition path sampling study, J. Phys. Chem. B. 117 (2013) 1419-1428.

[6]. J.P. Ryckaert, G. Ciccotti, H.J.C. Berendsen, Numerical integration of the cartesian equations of motion of a system with constraints: molecular dynamics of n-alkanes, J. Comput. Phys. 23 (1977) 327-341.

[7]. S. Chowdhuri, A. Chandra, Molecular dynamics simulations of aqueous NaCl and KCl solutions: effects of ion concentration on the single-particle, pair, and collective dynamical properties of ions and water molecules, J. Chem. Phys. 115 (2001) 3732-3741.

[8]. S. Chowdhuri, A. Chandra, Hydration structure and diffusion of ions in supercooled water: ion size effects, J. Chem. Phys. 118 (2003) 9719-9725.

[9]. J.V.L. Beckers, C.P. Lowe, S.W. De Leeuw, An iterative PPPM method for simulating Coulombic systems on distributed memory parallel computers, Mol. Simulat. 20 (1998) 369-

383.

[10]. S. Plimpton, Fast parallel algorithms for short-range molecular dynamics, J. Comput. Phys. 117 (1995) 1-19.

[11]. S. Nosé, A unified formulation of the constant temperature molecular dynamics methods, J. Chem. Phys. 81 (1984) 511-519.

[12]. W.G. Hoover, Canonical dynamics: equilibrium phase-space distributions, Phys. Rev. A. 31 (1985) 1695-1697.

[13]. W.C. Swope, H.C. Andersen, P.H. Berens, K.R. Wilson, A computer simulation method for the calculation of equilibrium constants for the formation of physical clusters of molecules: Application to small water clusters, J. Chem. Phys. 76 (1982) 637-649.

[14]. E. Ahadi, L. Konermann, Modeling the behavior of coarse-grained polymer chains in charged water droplets: Implications for the mechanism of electrospray ionization, J. Phys. Chem. B, 116 (2012) 104-112.

[15]. N. Bjerrum, Untersuchungen über Ionenassoziation. Det Kgl. Danske Videnskabernes Selskab. Mathematisk-fysisike Meddelelser, VII, 9 (1926).

[16]. B.B. Wang, X.D. Wang, T.H. Wang, D.J. Lee, Size control mechanism for bio-nanoparticle fabricated by electrospray deposition, Dry. Technol. 33 (2015) 406-413.

Table and Figure Captions

Table 1. Values of potential parameters.

Figure 1. Schematic of the simulation system.

Figure 2. Snapshots from the simulation during evaporation of aqueous nano-film at the absence of the electric field.

Figure 3. (a) Number of evaporated water molecules and (b) Evaporation rate versus time for aqueous film at various electric fields.

Figure 4. Number of evaporated water molecules versus time for pure water nano-film at various electric fields.

Figure 5. Average kinetic energy of liquid water molecules versus time for (a) water film and (b) aqueous film at the various electric fields.

Figure 6. Average kinetic energy of (a) Na^+ and (b) Cl^- versus time for aqueous film at various electric fields.

Figure 7. Time evolutions of average potential energy of liquid water molecules in (a) pure water film and (b) aqueous film at the various electric fields.

Figure 8. Number of water molecules evaporated versus time for aqueous film at various directions of electric field.

Figure 9. Average kinetic energy of (a) Na^+ and (b) Cl^- versus time for aqueous film at various directions of electric fields.

Figure 10. (a) Schematic of the simulation system for the thicker aqueous nano-film. (b) Number of water molecules evaporated versus time for aqueous film at various directions of electric field.

Table 1. Values of potential parameters.

Particles *i*,*j*	$\sigma_{i,j}$(Å)	$\varepsilon_{i,j}$(eV)	*q* (e)
Na^+-Na^+	2.5830	0.0043	+1.0000
Cl^--Cl^-	4.4000	0.0043	-1.0000
O-O	3.1660	0.0067	-0.8476
H-H	0.0000	0.0000	+0.4238
Na^+-Au	2.8745	0.0444	——
Cl^--Au	3.4845	0.0444	——
O-Au	2.8675	0.0554	——
H-Au	0.0000	0.0000	——

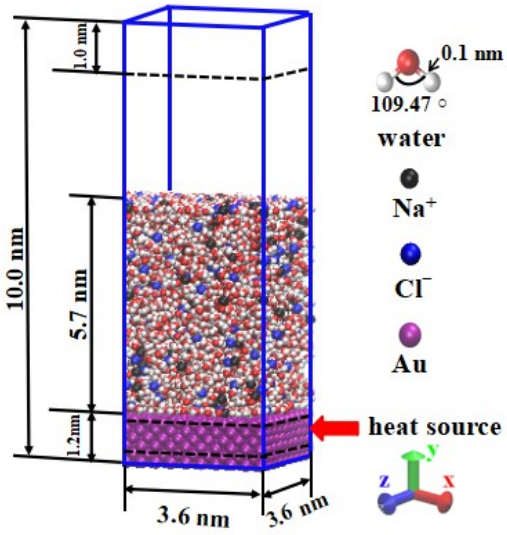

Figure 1. Schematic of the simulation system.

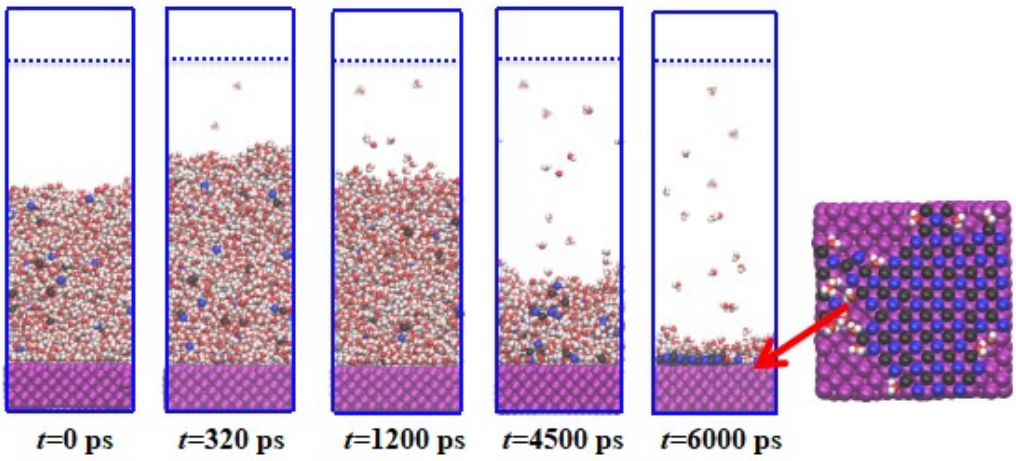

Figure 2. Snapshots from the simulation during evaporation of aqueous nano-film at the absence of the electric field.

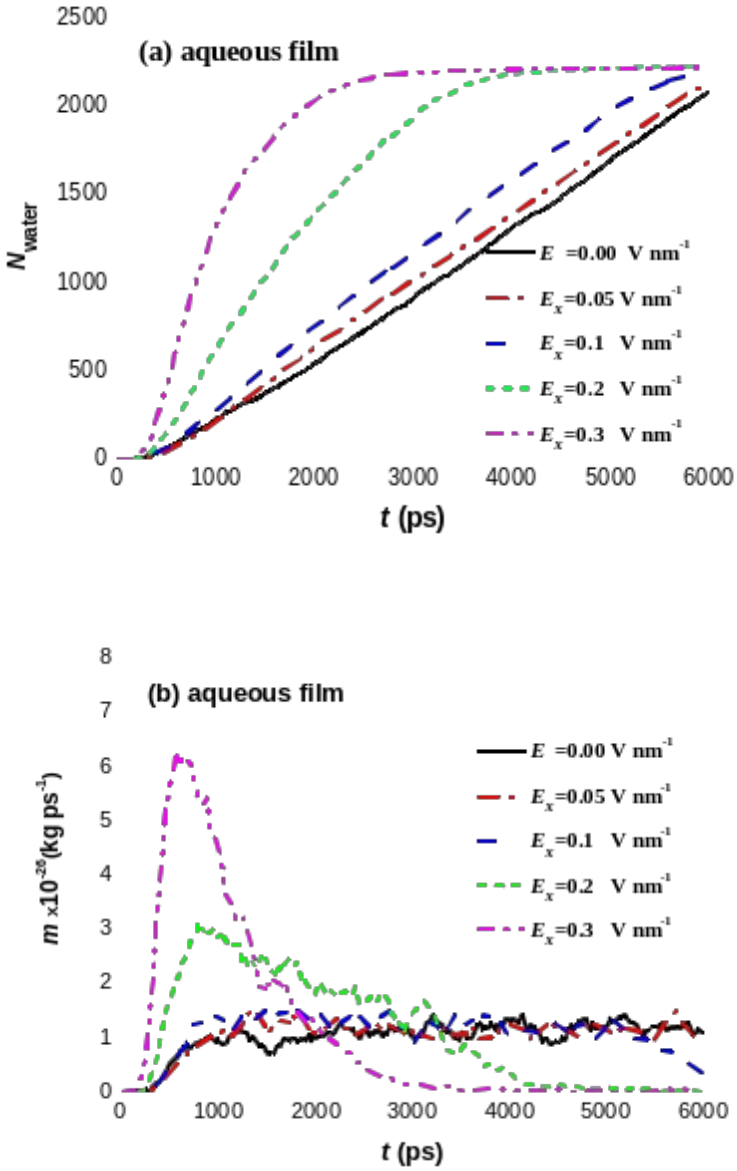

Figure 3. (a) Number of evaporated water molecules and (b) Evaporation rate versus time for aqueous film at various electric fields.

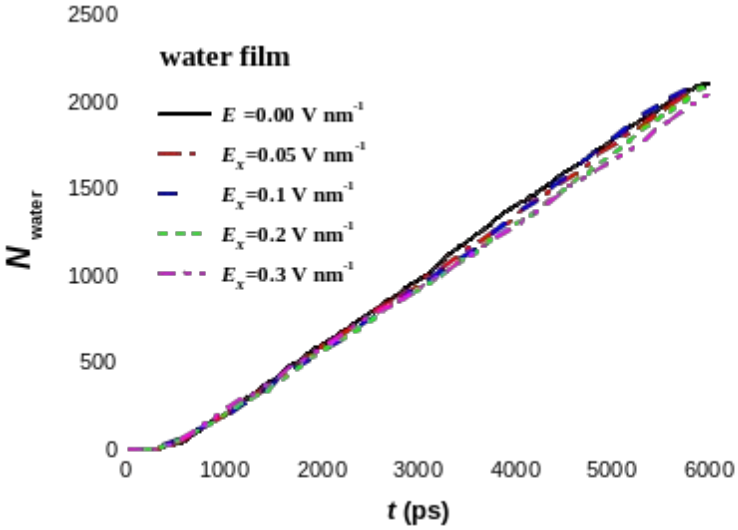

Figure 4. Number of evaporated water molecules versus time for pure water nano-film at various electric fields.

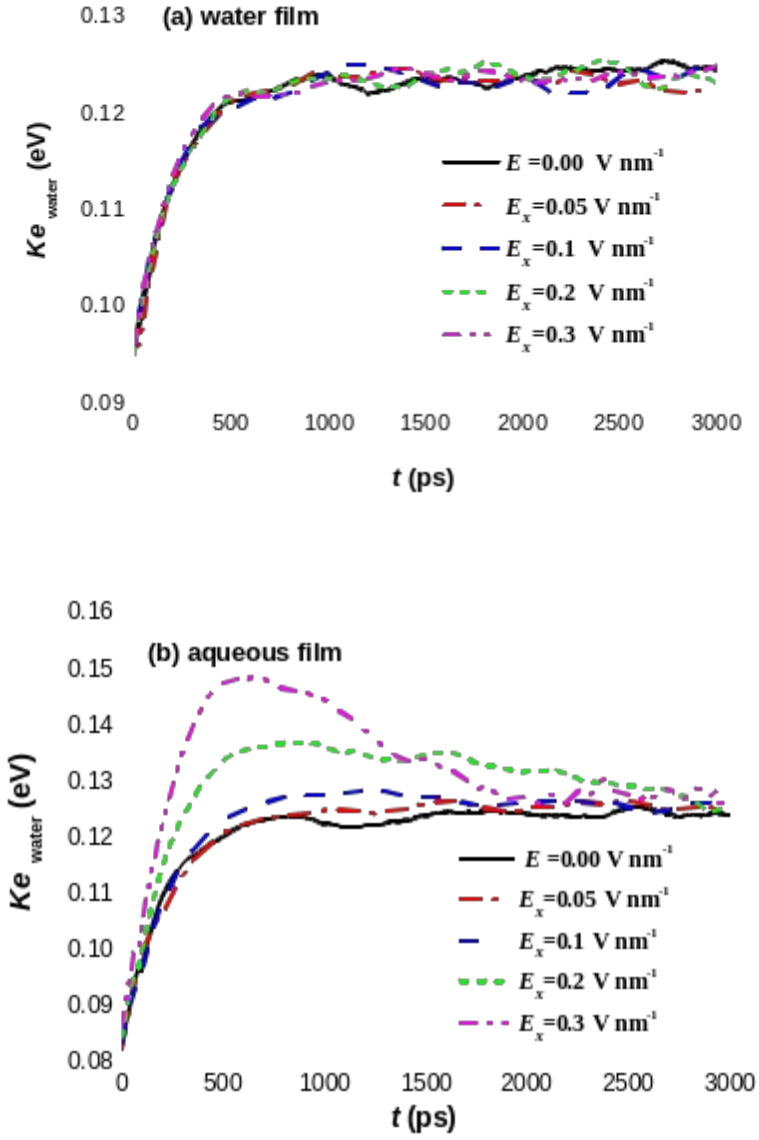

Figure 5. Average kinetic energy of liquid water molecules versus time for (a) water film and (b) aqueous film at the various electric fields.

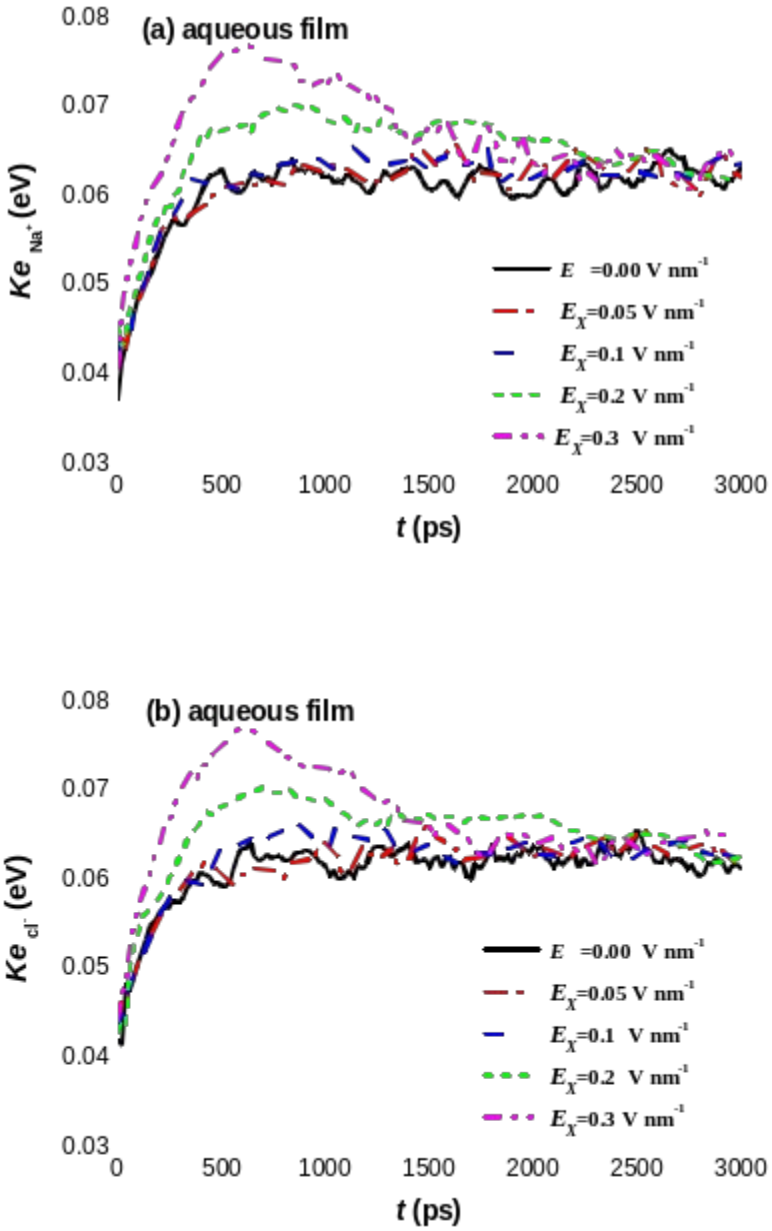

Figure 6. Average kinetic energy of (a) Na^+ and (b) Cl^- versus time for aqueous film at various electric fields.

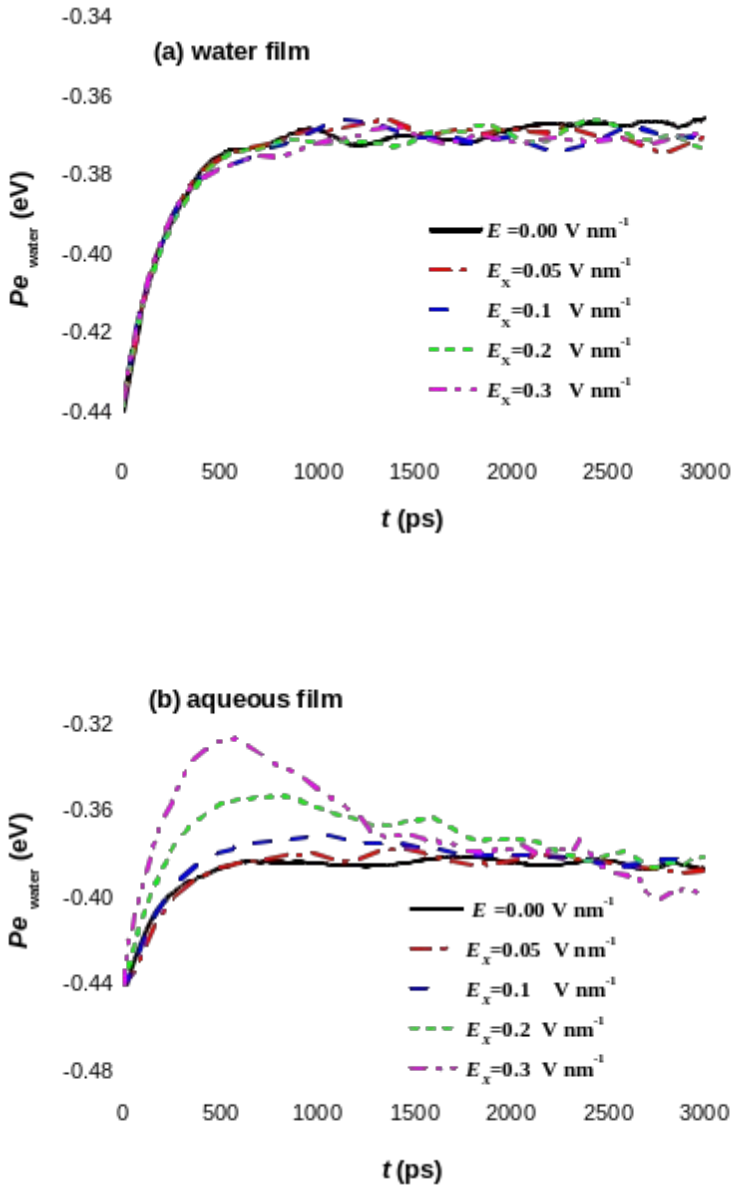

Figure 7. Time evolutions of average potential energy of liquid water molecules in (a) pure water film and (b) aqueous film at the various electric fields.

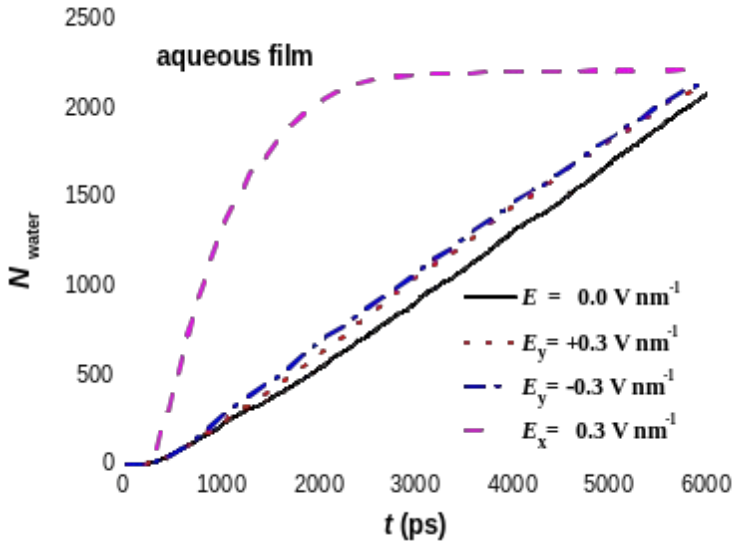

Figure 8. Number of water molecules evaporated versus time for aqueous film at various directions of electric field.

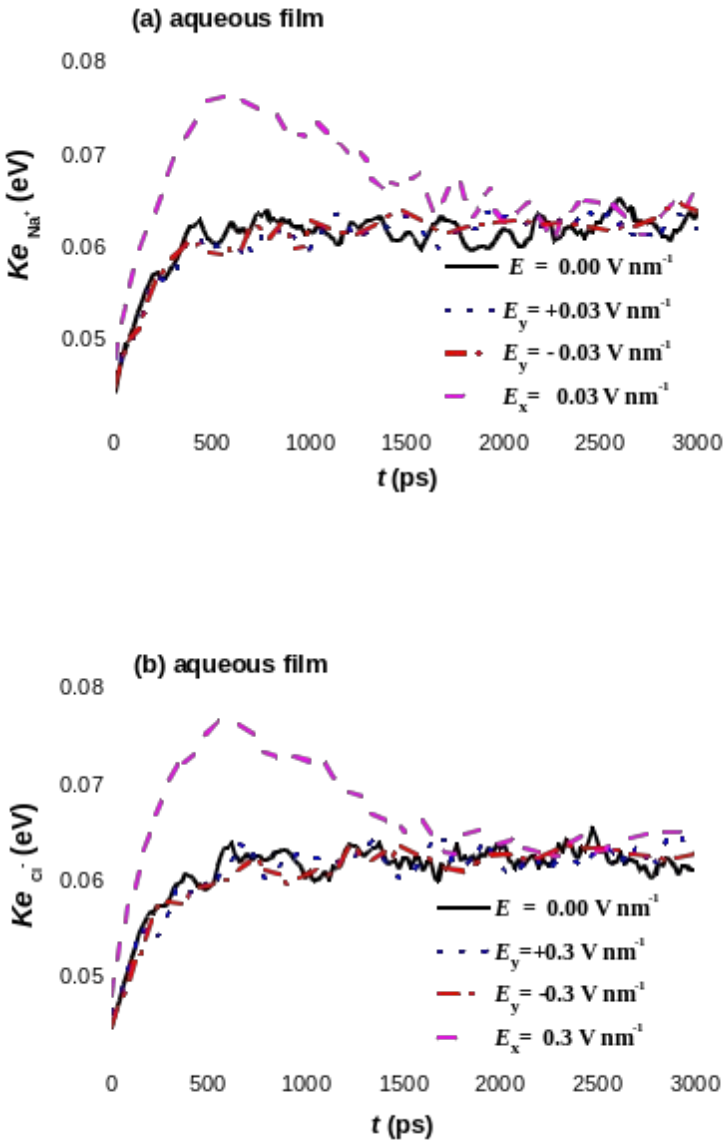

Figure 9. Average kinetic energy of (a) Na^+ and (b) Cl^- versus time for aqueous film at various directions of electric fields.

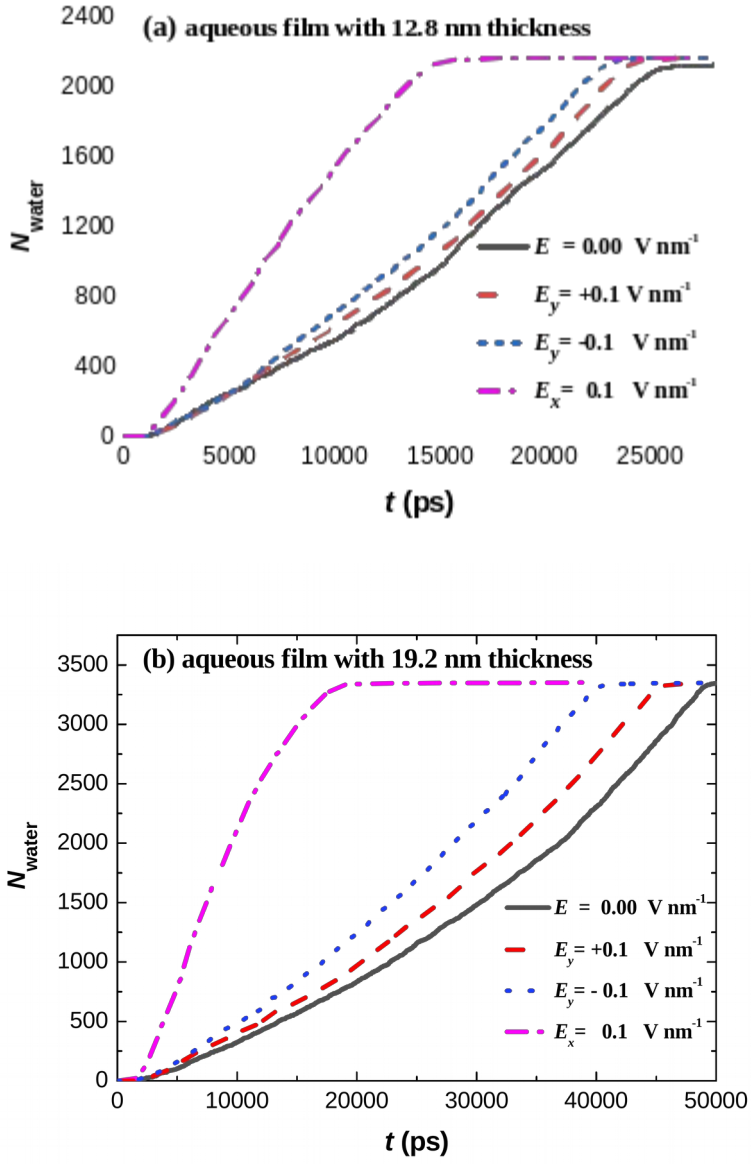

Figure 10. Number of water molecules evaporated versus time for the aqueous film with (a) 12.8 nm and (b) 19.2 nm thickness at various directions of electric field.